On Solitary Waves in the Atmosphere

D. R. CHRISTIE, K. J. MUIRHEAD AND A. L. HALES

Research School of Earth Sciences, The Australian National University, Canberra, A.C.T., 2600

(Manuscript received 20 January 1977, in final form 18 November 1977)

ABSTRACT

This paper is concerned with a description and interpretation of two unusual types of isolated atmospheric gravity wave observed near Tennant Creek in central Australia. These waves occur in the form of solitary waves of elevation and solitary waves of depression. Comparison of experimental data with theory leads to the conclusion that the majority of the observed isolated waves of elevation belong to the class of deep-fluid internal solitary waves considered by Benjamin and by Davis and Acrivos. The second fundamentally different type of large-amplitude isolated wave is tentatively identified as a classical solitary wave of depression.

A brief discussion is given of a number of possible source mechanisms which may give rise to internal solitary atmospheric waves. It is proposed that the following two dynamical processes play an important role in the creation of solitary atmospheric waves in the arid interior of Australia: 1) the interaction of nocturnal katabatic density currents with an existing radiation inversion; and 2) the interaction of a propagating horizontal sea breeze vortex with the nocturnal inversion.

1. Introduction

It is well known that the creation, propagation and dissipation of gravity waves play an important role in the dynamics of the earth's atmosphere. The reasons for studying long-period waves of this type are therefore twofold: in the first place, an understanding of the initial disturbance which gives rise to these waves, the mechanisms by which they propagate and their dispersion characteristics provide insight into the fundamental nature of atmospheric fluid mechanics; second, it seems to be equally important to understand the influence that the passage of these waves has on the development of local meteorological conditions—for example, gravity waves may sometimes be correlated with the release of latent atmospheric instabilities which in turn give rise to such diverse phenomena as clear-air turbulence, severe convective storms and, possibly, in the extreme case the development of tornado activity.

The purpose of this paper is to present a description and interpretation of the results of an experimental investigation of large-amplitude isolated propagating atmospheric disturbances which have been observed, using an array of high-sensitivity microbarometers, at the Warramunga Seismic Station located near Tennant Creek in central Australia. It is thought that these unusual phenomena which occur as isolated waves of elevation and isolated waves of depression represent two new types of naturally occurring internal solitary wave. In particular, it will be shown that the properties of the waves of elevation are in accord with the class of deep-fluid solitary waves considered by Benjamin (1967) and by Davis and Acrivos (1967) and that the internal waves of depression appear to be described by the classical solitary wave theories of Peters and Stoker (1960), Long (1965) and Benjamin (1966).

The properties of atmospheric waves have recently been reviewed by Gossard and Hooke (1975). In their most common form, horizontally propagating gravity waves in the troposphere occur as long-period, nearly sinusoidal wavetrains. This familiar form of atmospheric wave may be contrasted with an example of the specific type of unusual isolated wave considered in this paper as illustrated in the Tennant Creek microbarograph array record section shown in Fig. 1 for the late evening hours of 2 December 1976. Perhaps the most interesting feature of the observed isolated waves is their unusually large relative amplitude. A study of the properties of these waves therefore encompasses an investigation of the role of nonlinearity in large-scale fluid motions and an investigation of the process of wave-induced turbulence. It must be anticipated that this class of waves will prove to be important in other areas of geophysical fluid mechanics.

2. The internal solitary atmospheric wave

The phenomenon of the solitary wave, by its essentially nonlinear nature, occupies a unique place in the development of the theory of wave propagation in fluids. A classical wave of this type is usually defined (Lamb, 1932, Section 252) as a wave of single elevation which propagates at uniform velocity without change

0022-4928/78/0805-0825$10.50

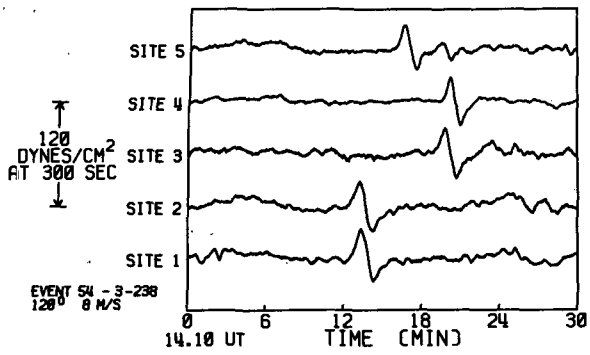

FIG. 1. An example of a microbarograph array record section corresponding to the passage of an internal solitary wave of elevation. The azimuth noted for this wave is the source direction measured from true north.

of form. The existence of these stationary waves may be viewed as being the consequence of equilibrium between the competing effects of nonlinearity and dispersion; that is, they arise from a balance between the tendency of waves to steepen ahead of their crests (amplitude dispersion) and the tendency of the longer period Fourier components to propagate at higher velocities (frequency dispersion).

The classical solitary wave of elevation was first observed by Scott-Russell (1837, 1844) on the free surface of shallow water of uniform depth. Subsequently, Boussinesq (1871) and Rayleigh (1876) independently derived approximations for the speed of propagation c and the form $\eta(x)$ of the wave profile at the free surface. These authors found, to first order in the relative amplitude $\alpha=a/h$, a solitary wave solution described by

$$\eta(x)=a\,\mathrm{sech}^2\left[\frac{(3\alpha K)^{\frac{1}{2}}}{2}\frac{x}{h}\right], \tag{2.1a}$$

$$c=[gh(1+\alpha)]^{\frac{1}{2}}, \tag{2.1b}$$

where h is the undisturbed fluid depth, a the maximum amplitude of the wave and g the acceleration due to gravity. A measure of the effective wavelength of these waves is given by the full width of the wave profile at half maximum, i.e.,

$$w_{\frac{1}{2}}=\frac{4\ln(1+2^{\frac{1}{2}})}{(3\alpha K)^{\frac{1}{2}}}h. \tag{2.1c}$$

In the Boussinesq approximation the factor K in the argument of the hyperbolic secant takes the value $K=1$, while in the solution found by Rayleigh $K=(1+\alpha)^{-1}$.

These early investigations revealed an important property of solitary waves; that is, they are always supercritical—the speed of propagation always exceeds the speed

$$c_0=(gh)^{\frac{1}{2}} \tag{2.2}$$

of infinitesimal long waves. This property may be expressed to first order in the dimensionless amplitude as

$$F^2=1+\alpha>1, \tag{2.3}$$

where F is the Froude number. It should be noted that all forms of the classical solitary wave are characterized by fluid systems in which the horizontal length scale of the motion is long compared to the total fluid depth.

Korteweg and de Vries (1895) showed that the time evolution of small but finite dispersive shallow-water waves is described, in the first approximation, by a nonlinear partial differential equation (the KdV equation) which may be written as

$$\frac{\partial\eta}{\partial t}+c_0(1+\epsilon\eta)\frac{\partial\eta}{\partial x}+c_0\beta\frac{\partial^3\eta}{\partial x^3}=0, \tag{2.4}$$

where $\epsilon=\frac{3}{2}$ h and $\beta=h^2/6$. From this equation they were able to demonstrate the existence of a class of periodic long waves of finite amplitude and permanent form which are described by the square of the Jacobi elliptic function cn of modulus k. In particular, they showed that these waves, which they called *cnoidal* waves, reduce to the classical solitary wave of finite extent in the limit as the wavelength goes to infinity. Despite this progress, it was not until relatively recently that Lavrent'ev (1964) and Friedrichs and Hyers (1954) succeeded in rigorously proving the mathematical existence of a solitary wave solution of the full nonlinear equations.

There have been a number of attempts to improve on the first-order approximation to the classical solitary wave. The second-order solution was found by Laitone (1960), the third-order by Grimshaw (1971), and a fifth-order expression for the wave speed has been given by Long (1956b). Much of the recent work on classical solitary waves has concentrated on the determination of the solitary wave of maximum height. Estimates have been obtained from an exact calculation of the position of points on the profile of the wave of maximum amplitude (Yamada, 1957; Yamada *et al.*, 1968), from an extrapolation of a ninth-order series approximation for the profile of waves of less than maximum amplitude (Fenton, 1972), from an extrapolation of the results of a finite-difference formulation of the problem (Chan, 1974), and from the solution of an integral equation (Lenau, 1966; Byatt-Smith, 1970; Strelkoff, 1971). A puzzling aspect of these calculations has been the small, but significant, discrepancy between the various estimates for the wave of maximum amplitude. This problem has recently been resolved by Longuet-Higgins and Fenton (1974) who found that the wave of maximum height does not correspond—as had generally been assumed—to the wave of maximum speed. According to these authors the wave of maximum amplitude is specified by

$$\alpha_{\max}=0.827, \quad F=1.286, \tag{2.5}$$

in good agreement with the results of Yamada (1957) and Lenau (1966), while the wave of maximum speed corresponds to

$$\alpha=0.790, \quad F_{max}=1.294.$$

It is worth noting that the Boussinesq approximation (2.1) to the shape of the classical solitary wave compares favorably with the exact profiles computed by Yamada (1958) and by Byatt-Smith (1970) provided the non-dimensional amplitude α is less than about 0.7.

The theoretical study of internal solitary waves, i.e., waves which exist as a consequence of internal density stratification, was initiated by Keulegan (1953) who considered a system of two superimposed liquids of different constant densities, bounded above and below by rigid surfaces. Long (1956b) and Benjamin (1966) have also investigated this particular model. Using a systematic perturbation procedure developed by Friedrichs (1948) and Keller (1948), Abdullah (1956) obtained a first-order solution for the classical internal solitary wave at the interface of a two-layer atmosphere subject to the condition that the hydrostatic law holds for the upper layer; that is, that motion of the free surface can be neglected. This solution is a supercritical wave of elevation described by the Boussinesq approximation (2.1) with the expression for the phase velocity modified to

$$c=c_0'(1+\tfrac{1}{2}\alpha), \tag{2.6}$$

where the infinitesimal internal wave critical speed is now given by the reduced form

$$c_0'=(g'h)^{\frac{1}{2}}, \tag{2.7}$$

where

$$g'=g(\rho_1-\rho_2)/\rho_1 \tag{2.8}$$

and ρ_2 and ρ_1 are the densities of the upper and lower fluids, respectively.

A more general treatment of internal solitary waves has been given by Peters and Stoker (1960). They examined the full problem of a two-fluid system with a free upper boundary as well as the more difficult problem of the existence of internal solitary waves in a fluid whose density decreases exponentially with height. In the case of the two-fluid problem they found two types of solitary-wave solution corresponding to two critical speeds given by

$$c_0^s=[\tfrac{1}{2}gh_1(1+R+q)]^{\frac{1}{2}}, \tag{2.9a}$$

$$c_0^i=[\tfrac{1}{2}gh_1(1+R-q)]^{\frac{1}{2}}, \tag{2.9b}$$

with

$$q=[(1-R)^2+4(\rho_2/\rho_1)R]^{\frac{1}{2}},$$

where $R=h_2/h_1$ and h_2 and h_1 are the respective depths of the upper and lower fluids in the region of undisturbed flow. The first of these solutions has maximum amplitude at the free surface and represents the equivalent of the ordinary classical solitary wave of elevation; the second describes an internal solitary wave with a maximum amplitude at the interface much larger than the amplitude at the surface. The internal solitary wave may be either a wave of depression or a wave of elevation. If the difference in the two fluid densities is small, then the streamlines are lines of elevation at the interface if $R>1$ and lines of depression if $R<1$. This form of the two-fluid solution may be suited to a description of large-scale internal atmospheric solitary waves. For this particular model, the wave profile at the interface is given by the usual classical solitary waveform (2.1) with

$$K=\left|\frac{(R-1)}{R^2}\right| \tag{2.10a}$$

and the corresponding internal critical speed reduces to

$$c_0^i=\left[g\left(1-\frac{\rho_2}{\rho_1}\right)\frac{h_1h_2}{(h_1+h_2)}\right]^{\frac{1}{2}}. \tag{2.10b}$$

In the case of a fluid of finite depth with a density distribution which decreases exponentially upward, Peters and Stoker found an infinite number of possible internal solitary wave modes corresponding to an infinite spectrum of internal critical speeds. This problem has also been investigated by Long (1965), and in an elegant and very general treatment of the subject of internal solitary waves in shallow fluids by Benjamin (1966). The general solitary wave solutions in this case are complicated and will not be given here; it is noted, however, that according to Benjamin, for the case of a free upper boundary, the solitary wave mode corresponding to the highest critical speed—predominantly a wave of depression—is probably the most significant mode in fluids of this type.

Up to this point this discussion has been limited to a consideration of internal solitary waves which can exist in fluids of finite depth. Benjamin (1967) and Davis and Acrivos (1967) have independently presented the results of a theoretical and experimental investigation of an entirely new class of internal solitary waves which can exist in fluids of great depth. These new types of internal waves are shown to exist in regions where the fluid density varies only within a layer of thickness h which is much smaller than the total fluid depth and smaller than the effective horizontal length scale λ characteristic of the solitary wave. Thus, in stratified fluids of great depth, the fundamental scale against which wave dimensions are to be measured is the thickness of the region of significant density variation rather than the total fluid depth.

For a two-fluid system in which the upper fluid extends to infinity over a lower fluid of depth h resting on a horizontal rigid surface, Benjamin finds a solitary wave solution of the form

$$\eta(x)=\frac{a\lambda^2}{x^2+\lambda^2}, \tag{2.11a}$$

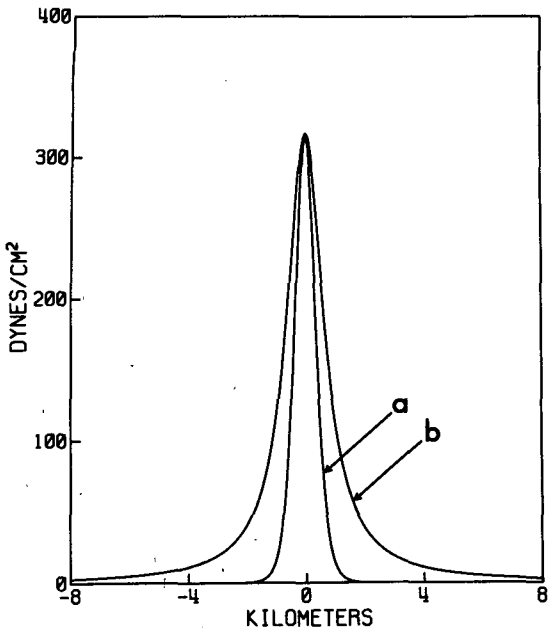

FIG. 2. Internal solitary wave surface pressure profiles corresponding to a 5°C temperature inversion at the 980 mb level. The dimensionless amplitude α is chosen to be 0.5. (a) Classical internal solitary wave described by (2.1) with $K=1$. (b) Internal solitary wave described by Benjamin's theory (2.11) for a fluid of great depth.

with

$$c=c_0'(1+\tfrac{3}{4}\alpha)^{\frac{1}{2}}, \tag{2.11b}$$

where

$$2\lambda=w_{\frac{1}{2}}=\frac{8}{3}\frac{\rho_1 h}{\rho_2 \alpha}, \tag{2.11c}$$

c_0' is the reduced internal wave critical speed given by (2.7), and ρ_2 and ρ_1 are the densities of the upper and lower fluids, respectively.

Benjamin has also considered the problem of a shallow fluid with an exponential density gradient in contact with a deep fluid of constant density and, further, the more general problem of solitary waves associated with a thin transition region contained between two homogeneous fluids of substantial depth. In direct analogy with the shallow fluid theory, the continuous variation in density is shown to give rise to an infinite set of solitary-wave modes. For the case of a thin region of sudden vertical density variation in a stably stratified system, the lowest order mode solitary-wave solution takes the form of a bulge which propagates along the interface. This interesting result has been confirmed in the laboratory experiments of Davis and Acrivos (1967) and Hurdis and Pao (1975). The experiments and numerical calculations of Davis and Acrivos are particularly interesting in that they show that solitary waves of this type can exist with dimensionless amplitude near 2.0 and that waves with large amplitudes exhibit an unusual closed circulation in the streamline pattern which suggests the presence of a propagating vortex pair.

It was long thought that solitary waves would only be produced as a consequence of rather specialized initial conditions. The discovery by Zabusky and Kruskal (1965) that the solitary wave or *soliton* solutions of the KdV equation (2.4) possess the remarkable linear property of preserving their form following nonlinear interaction has provided in recent years a great deal of impetus to the study of the general properties of the nonstationary solutions of the KdV equation and other nonlinear wave equations known to admit soliton solutions (see, e.g., Karpman 1975). The importance of these results to the study of atmospheric fluid mechanics stems principally from the fact that soliton production in density-stratified fluids is now known to occur under widely varying initial conditions.

We now consider the existence of solitary-wave motions in the atmosphere. It would seem, on the basis of the atmospheric scale involved, that the deep-fluid solitary-wave solution (2.11) found by Benjamin (1967) is best suited to a simple description of solitary waves in the planetary boundary layer, while classical internal solitary-wave theory should provide a reasonable description of higher altitude waves.

In order to clarify the interpretation of experimental data we consider the properties, as predicted by both the classical and deep-fluid theories, of internal solitary waves associated with a density discontinuity at the 980 mb (280 m) level corresponding to a temperature inversion of 5°C. The air beneath the inversion is taken to have a mean temperature of 270 K and the dimensionless amplitude α of the wave is chosen to have a value of 0.5, corresponding to a wave with amplitude less than maximum. With these conditions, a classical internal solitary wave as described by the theory of Abdullah [Eqs. (2.1) and (2.6) with $K=1$] would propagate along the inversion at a speed of 8.9 m s^{-1} with a full width at half maximum, $w_{\frac{1}{2}}$, of 0.81 km and would produce, assuming the hydrostatic approximation, a maximum pressure perturbation ΔP at ground level of 317 dyn cm^{-2}; in contrast, the classical theory of Peters and Stoker [Eqs. (2.1) and (2.10) with $K\ll 0.1$] describes an internal solitary wave which propagates with nearly the same velocity but with a much larger effective wavelength. Alternatively, for the same wave amplitude, Benjamin's deep-fluid theory (2.11) describes a solitary wave with $w_{\frac{1}{2}}=1.52$ km propagating at a speed of 8.4 m s^{-1}. It is, of course, unlikely that the classical treatment of the theory provides an accurate description of internal solitary waves whose characteristic horizontal dimensions, as in this example, are much smaller than the total fluid depth.

A comparison of the classical and deep-fluid solitary-wave profiles for an inversion at the 980 mb level is shown in Fig. 2. Note that, as a consequence of an

asymptotic exponential behavior, the influence of the classical wave is much more localized than that of the deep-fluid wave of elevation. The shape of both types of solitary wave depends on the value of the dimensionless amplitude α; as α increases the wave profile narrows and the curvature at the crest increases until at maximum amplitude the peak is reduced in accordance with Stokes's (1880) conjecture[1] to a cusp enclosing an angle of 120°.

The possible existence of atmospheric internal solitary waves was suggested by Abdullah (1949). The only direct evidence for atmospheric solitary waves appears to be the description by Abdullah (1955) of a large-amplitude propagating disturbance which appeared over Kansas during the early daylight hours of 29 June, 1951. This disturbance, which produced a ground level pressure perturbation of 3.4 mb, took the form of an elevated mass of cold air propagating on an inversion at a height of about 2 km. The elevated disturbance appeared to extend over about 150 km and was observed to travel with approximately constant form at speeds between 18 and 24 m s^{-1} over a distance of about 800 km. Abdullah concluded that this disturbance represented a classical internal solitary wave of elevation and attributed its formation to the impulsive movement of a quasi-stationary cold front into the layer of inversion. As can be seen from the following description, most of the atmospheric solitary waves observed at Tennant Creek which belong to the class of isolated waves of elevation have an effective wavelength of only a few kilometers; they therefore appear to be entirely different from the single observation described by Abdullah. It will be shown that the properties of this new form of isolated wave are best described by the deep-fluid solitary-wave theory. In addition, a description will be given of observations of large-scale solitary waves of depression. An examination of the properties of this second new type of solitary wave indicates that these waves are probably best described classical solitary waves which propagate in a stratified fluid whose density decreases continuously with height.

Smart (1966) and Jordan (1972) have reported observations of "exponential pressure pulses" near Denver, Colo., which may represent a form of internal solitary wave. Additional evidence for the existence of solitary atmospheric waves based on observations of the pressure field is scarce. Phillips (1976) has described an interesting example of an isolated propagating disturbance which appeared as an exceptionally large pressure spike of 4 mb amplitude on barograph traces recorded on 25 March 1966 at El Adem and Tobruk in Libya. Apparently this disturbance was vigorous enough to trigger a seiche in Tobruk Harbor. It seems reasonable to assume that this disturbance and other smaller disturbances of a similar nature observed on the same day can be described as large-amplitude solitary waves of elevation.

At this point we would like to draw attention to two important acoustic radar studies which were carried out several years ago in areas of Australia with environments which are very similar to the semi-desert environment of the Warramunga Seismic Station. As will be seen, these studies provide considerable insight into the nature of the isolated propagating disturbances observed near Tennant Creek.

In a pioneering atmospheric acoustic sounding study McAllister *et al.* (1969) described an observation of a "weak, front-like" nocturnal disturbance characterized by the sudden appearance on the inversion level of a well-defined sharp spike in the sounder record. This initial pulse was followed by a rapid buildup of turbulence which, after a period of about 10 min, evolved into a pattern of reflections from distinct slowly ascending strata. A further feature of this record are the clearly visible large-amplitude vertical oscillations of the atmosphere in the wake of the initial spike. It is worth noting that the ratio of the amplitude of the initial pulse-like disturbance to the depth of the inversion both ahead of and immediately behind the pulse is at least as high as 1.0. It should also be emphasized that evidence of large-scale vertical atmospheric motions associated explicitly with the spike in the sounder record are provided by the corresponding records from the 75 m level of an instrumented tower which show that the passage of the disturbance corresponding to the spike produced a simultaneous negative pulse of 4°C in the temperature field and a positive pulse of about 6 m s^{-1} in the wind speed at this level. These observations were carried out during the month of June at Ivy Tanks on the edge of the arid Nullarbor Plain in South Australia.

A very interesting description of a series of acoustic sounding experiments which were carried out, again during the month of June, at Julia Creek, Queensland, has been given by Reynolds and Gething (1970). They also observed, usually under clear conditions with light surface winds, several examples of well-defined, very large-amplitude spikes on the interface of the nocturnal inversion. These unusual disturbances appear on the sounder record in two different forms: 1) a single clearly defined pulse with dimensionless amplitude of the order of unity which occurs along or immediately behind the leading edge of a rise in the height of the inversion and which is usually followed by patterns which indicate further wave activity near the inversion level; and 2) clusters of particularly large-amplitude pulses on the

[1] This conjecture, which has often been used as a limiting constraint in the mathematical development of large-amplitude wave theory, has recently been considered by Byatt-Smith and Longuet-Higgins (1976) as part of a study of the detailed shape of the profile of steep solitary waves. In all cases studied the maximum slope of the wave profile was less than 30°. However, the possibility that the maximum surface slope of the wave of highest amplitude exceeds the limit imposed by Stokes's criterion could not be excluded.

inversion level which precede a pattern of lower amplitude wavetrains—in this case, the sounder records indicate little evidence for a change in the height of the inversion. Note that the profiles of all of these spikes on the inversion are very similar in form to the profile of a deep-fluid solitary wave.

Reynolds and Gething have also described the corresponding measurements of temperature, wind speed and wind direction recorded at 15 m intervals to a height of 75 m on three towers separated by distances of the order of 40 km. A few of the essential features of these measurements are worth noting at this point. In the first place, the sounder measurement of the inversion height is in good agreement with the value determined from the tower measurements; there would therefore appear to be little doubt that the sounder records provide an accurate picture of the profile of disturbances on the inversion level. Second, an examination of the temperature structure associated with the isolated-pulse form of disturbance shows that by far the largest perturbation of the overall temperature field corresponds to the spike in the sounder record. This strongly suggests that this initial transient disturbance may be viewed as a distinct separate phenomenon and, as well, indicates that the dynamical processes associated with the pulse dominate the flow structure of the disturbance. At higher altitudes this initial perturbation takes the form of a strong negative temperature spike similar to that observed by McAllister *et al.*; at lower heights the amplitude of the spike decreases steadily with decreasing altitude and has almost disappeared from the trace recorded at 1.5 m. Note that this temperature distribution is consistent with the perturbations that would occur during the passage of a single large-amplitude internal wave of elevation associated with a density profile—as in the examples considered here—which decreases monotonically with height from the surface to the inversion level. Third, the observation of an apparently unattenuated disturbance at sites separated by about 40 km establishes that these pulses propagate over significant distances. These observations also reveal that the thermal structure associated with the spike in an isolated-pulse type of disturbance is identical in form to the structure associated with individual pulses in a cluster type of disturbance—this provides a convincing demonstration that the isolated pulses and the nonisolated pulses possess the same internal morphology, i.e., all of these events are manifestations of the same basic phenomena.

The essentially distinct nature of the pulselike disturbances is further indicated in the 75 m anemometer records which show a sudden temporary decrease in the wind speed from near 14 m s^{-1} to about 7 m s^{-1} during the passage of the pulse (in contrast to the observations of McAllister *et al.* where the pulse-associated wind showed an increase in speed) and a corresponding sudden temporary increase in the wind azimuth by about 60°. Note that this perturbation of the wind vector is significantly larger than any of the perturbations which occurred further on the disturbance.

Finally, it is worth noting the acoustic radar observation described by Shaw (1971) of a transient isolated disturbance in the atmospheric boundary layer which occurred near Melbourne in the early morning hours of 9 June 1970. This disturbance, which takes the form of a single symmetrical wave of elevation, appears to be very similar to the deep-fluid solitary wave described by the theory of Benjamin (1967).

During the course of the experiments at Tennant Creek we have observed a wide variety of unusual propagating lower tropospheric disturbances, many of which bear a close resemblance to the series of observations reported by Reynolds and Gething (1970) and to the events described by McAllister *et al.* (1969) and Shaw (1971). Observations have been made of disturbances in the form of smooth shallow internal density currents, complex solitary-wave families superimposed along the leading edge of sustained internal density flows, isolated clusters of solitary waves of elevation, and disturbances in the form of individual solitary waves propagate along the nocturnal inversion. It is thought that all of these disturbances belong to the class of deep-fluid nonlinear propagating disturbance described by the theory of Benjamin (1967). In particular, we identify all of the boundary layer pulse-like disturbances noted in the acoustic radar records and all isolated waves in the microbarograph array records which correspond to a transient increase in surface pressure as deep-fluid internal solitary waves of elevation. Since this paper is primarily concerned with the phenomenon of the atmospheric solitary wave we include here only those observations which clearly illustrate the basic features of isolated solitary waves and isolated clusters of solitary waves which propagate along an atmospheric inversion. It should be emphasized, however, that the available experimental evidence indicates that the genesis of the deep-fluid solitary waves described in this paper may often be traced to the evolution of the observed density-flow disturbances. Since the properties of these complex density currents constitute a separate area of investigation, a detailed description and interpretation of these unusual flow phenomena will be published separately.

3. Experimental arrangement and data processing techniques

The Warramunga Seismic Station is situated 37 km south-southeast of Tennant Creek. The centered quadrilateral array of microbarometers is located on slowly undulating semi-desert terrain at an elevation of about 410 m MSL with relief in the area encompassed by the array rising to a maximum of about 6 m. Probably the most important topographical features, insofar as the location of this array is concerned, are the

600 m Murchison and Davenport Ranges which run from 20 to 160 km to the south-southeast and the 1600 m Macdonnell Ranges, 450 km to the south. All of the area within 400 km to the west of the array can be described as semi-featureless stoney desert and an extensive dry steppe area known as the Barkly Tablelands forms the northeast quadrant.

Each element of the array consists of a National Bureau of Standards designed capacitor microphone which measures variations in pressure relative to a reference volume coupled through a high acoustic resistance to the atmosphere. The configuration of the infrasonic array along with the location of a vault containing a vertical long-period seismometer which is operated in conjunction with the infrasonic experiment are illustrated in Fig. 3. An array of Daniels noise-reducing space filters arranged in the form of a cross with the microbarograph inlet port at the center has been installed at each site. These filters provide useful suppression of incoherent wind noise in the period range below about 20 s. The measured amplitude response of the microbarometers is shown in Fig. 4.

The response of the differential pressure sensing array elements as a function of period is given by

$$R(T)=\frac{A(T_1+T_2)iT}{T^2+(T_1+T_2)iT-T_1T_2}, \qquad (3.1)$$

with $T_1=1.95$ s, $T_2=48.7$ s and $A=77.99$ counts dyn^{-1} cm^{-2}. In this expression the coefficients T_1, T_2 and A have been determined from a least-squares analysis of the measured instrumental response. An examination of this expression shows that waveforms with fundamental components near $T_0=(T_1T_2)^{\frac{1}{2}}=9.7$ s pass through the infrasonic detection filters essentially undisturbed; in contrast, wave patterns with fundamental components of the order of T_2 undergo substantial differentiation in the detection process—this latter circumstance dominates the observation of the two

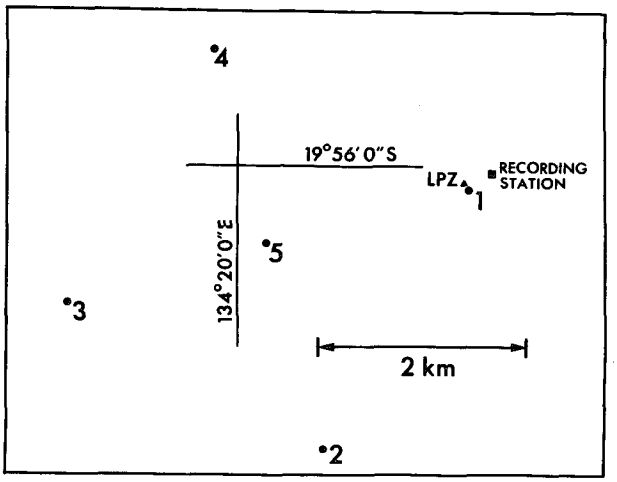

FIG. 3. Configuration of the five-component microbarograph array.

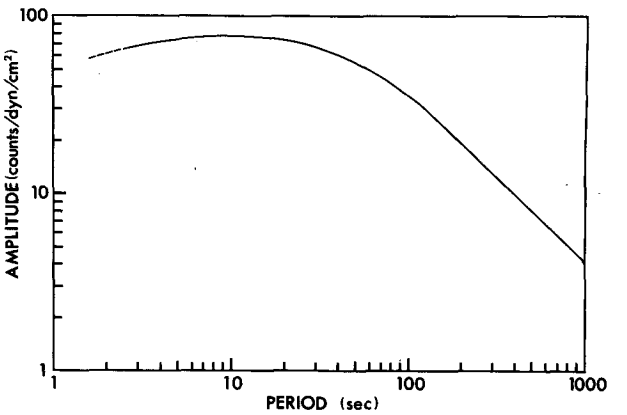

FIG. 4. Measured microbarograph amplitude response.

types of solitary-wave disturbance considered here. The influence of the instrumental response on the detection of solitary-wave surface pressure perturbations may be seen in the computed response to various forms of synthetic solitary wave data illustrated in Fig. 5. These patterns may be compared with the examples shown in Fig. 6 of the true surface pressure variation derived from recorded microbarograph data through an inversion of the instrumental response given by (3.1). As may be seen from these examples, solitary waves are easily identified in the output of the microbarograph array by their characteristic differential signature.

The five infrasonic channels and the vertical long-period seismometer channel are sampled at a rate of two samples per second, digitized via a 14-bit ADC and recorded in IBM compatible format on 7-track, 556 bpi tape. At the Australian National University these tapes are converted to 9-track, 800 bpi in a compact, two data word per 24-bit computer word format, which conserves magnetic tape and which is suitable for analysis on a 48K Harris Datacraft 6024/4 computer.

A SIAP S2000 meteorological station was installed at site 1 near the end of the recording period spanned by this work. This instrument provides a continuous record of surface temperature, wind speed, wind direction, rainfall and humidity. Accurate timing was achieved through the introduction of a chart marker activated by a pulse derived from the crystal-controlled digital time standard of the seismic station. The analysis of the meteorological data has not yet been completed. However, some of these data which are essential to the interpretation of the phenomena described here are included in this paper.

The main signal processing technique used on the array data consists of a beam-forming program which utilizes the nonlinear N-root method devised by Muirhead (1968). The output $e_i(t)$ of the ith array element is digitally filtered in the bandpass region of interest, properly phased by time shifting to correspond to the passage of a plane wavefront across the array, and then reduced to the Nth root with sign preserved.

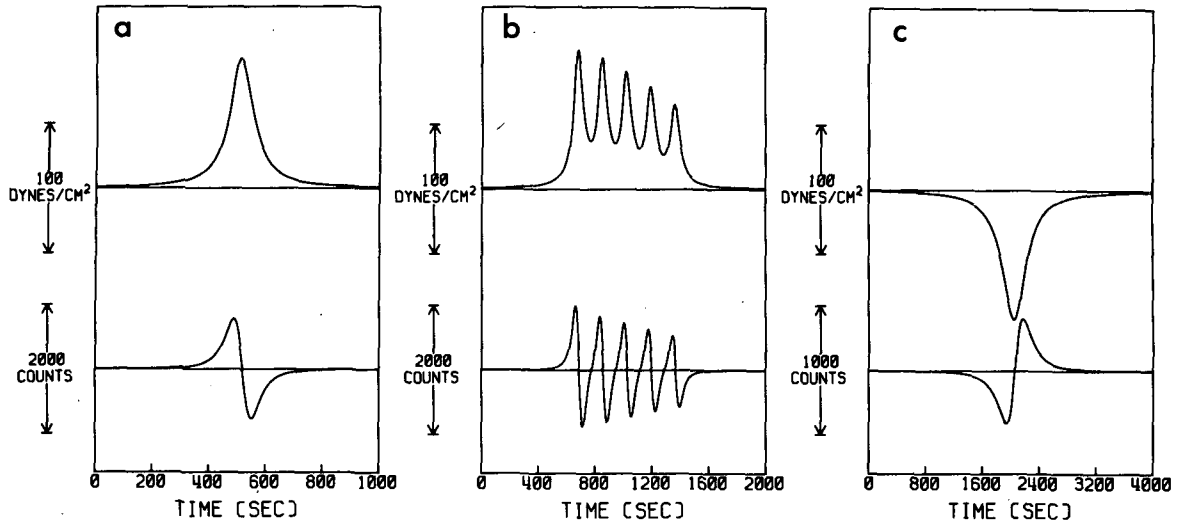

FIG. 5. Computed microbarograph response to synthetic micropressure waveforms for (a) solitary wave of elevation, (b) soliton wave packet ordered by amplitude and (c) solitary wave of depression.

The resulting product is summed over the n-element array to give

$$R_N(t) = \frac{1}{n} \sum_{i=1}^{n} |\bar{e}_i(t)|^{1/N} \operatorname{sign}[\bar{e}_i(t)], \tag{3.2}$$

where $\bar{e}_i(t)$ represents the filter output. This quantity is then raised to the Nth power with sign preserved to provide the signal statistic

$$S_N(t) = |R_N(t)|^N \operatorname{sign}[R_N(t)]. \tag{3.3}$$

The principal advantage of this type of automatic infrasonic array processing arises from the fact that this nonlinear beam-forming technique gives added weight to the presence of coherent energy in the spectrum. This has proven to be of value in the treatment of data from Tennant Creek due to the prevalence in this semi-desert environment of incoherent, essentially non-Gaussian noise such as that due to dust devils (small whirlwinds called *willy-willies* in Australia) which interact with only one sensor. It can be easily shown that large events of this type are suppressed in the output of the Nth root process by a factor of approximately n^{-N}.

All infrasonic data are processed for a value of $N=2$. This output is supplemented by a parallel determination of an integrated polarity stack over the phased array which corresponds to the Nth root process in the limit $N \to \infty$. Further details on the Nth root multichannel filter may be found in Kanasewich *et al.* (1973) and Muirhead and Ram Datt (1976).

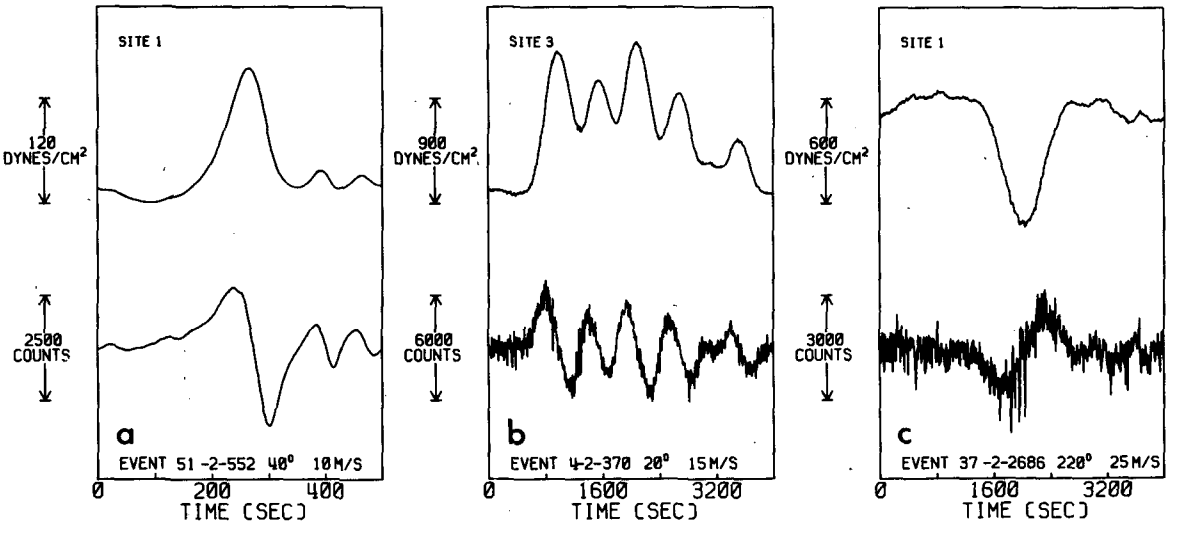

FIG. 6. Variation in surface pressure derived from recorded microbarograph data through an inversion of the instrumental response specified by (3.1) for (a) solitary wave of elevation, (b) soliton wave packet and (c) solitary wave of depression.

Power spectral estimates of the data are computed directly using the fast Fourier transform. In order to reduce the variance of the estimate the calculations are carried out using the method of time averaging over modified periodgrams described by Welch (1967). The digital time series t_r is divided into k portions t_{rj} each of length $M=2^{10}$ points; the elements in each segment j are then weighted according to a cosine taper data window d_r effective over the 10% limits of the segments, as suggested by Bingham *et al.* (1967), and transformed to the frequency domain to give

$$X_j(f)=\sum_{r=0}^{M-1} d_r t_{rj} \exp(-2\pi i r f/M). \qquad (3.4)$$

The power spectral density is then determined by averaging over the k segments,

$$\bar{P}(f)=(2\Delta t/kMU)\sum_{j=1}^{k}|X_j(f)|^2, \qquad (3.5)$$

where Δt is the sampling interval and the factor

$$U=(1/M)\sum_{r=1}^{M} d_r^2=0.875 \qquad (3.6)$$

preserves the invariance of the area under the spectrum to the influence of the data taper window. The power spectral estimates obtained in this way are converted to true spectral estimates by dividing by the square of the microbarograph amplitude response shown in Fig. 4.

4. Observations and interpretation

We first consider the properties of the isolated waves of elevation. A large number of disturbances of this type have been observed in over two years of continuous recording at the infrasonic array near Tennant Creek. These unique waves, which only occur at night, are reasonably well described by the deep-fluid solitary-wave theory outlined above. Consequently, as mentioned in the Introduction, these waves are interpreted as being examples of atmospheric internal solitary waves which propagate along the nocturnal inversion.

An examination of the microbarograph record inversions shows that, in general, these subsonic waves produce a symmetrical pulse-like perturbation in the atmospheric flow field characterized by an initial slow rise in surface pressure over a period of several minutes which gradually develops into an exponential increase leading to a fairly sharp but rounded crest. The microbarograph signatures corresponding to the passage of a wide variety of these commonly occurring buoyancy waves are illustrated in Figs. 7–12. The two relatively weak but well-defined isolated solitons illustrated in Fig. 7 are typical of the most commonly observed form waves. Occasionally (see Fig. 8b) large-amplitude isolated waves of elevation are observed to pass over the

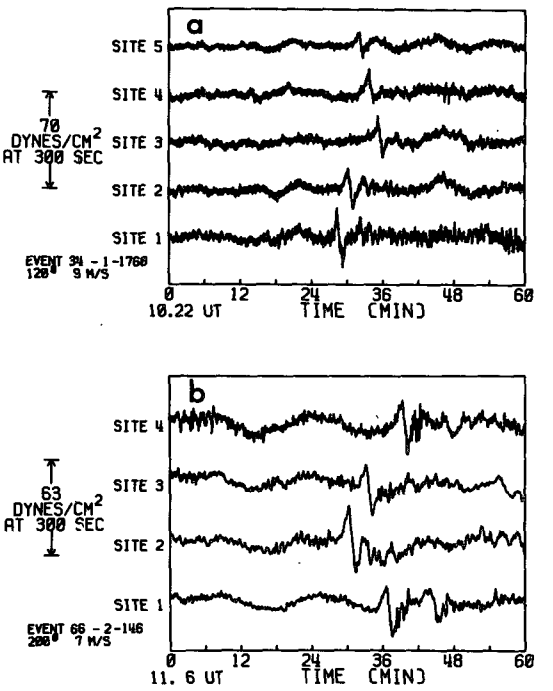

FIG. 7. Examples of solitary waves of elevation observed at the Warramunga Seismic Station. Despite the relatively poor signal-to-noise ratio these waves are clearly defined in the infrasonic records. The deep-fluid solidary-wave signals shown in this figure are typical of the large number of small-amplitude events of this type which have been observed.

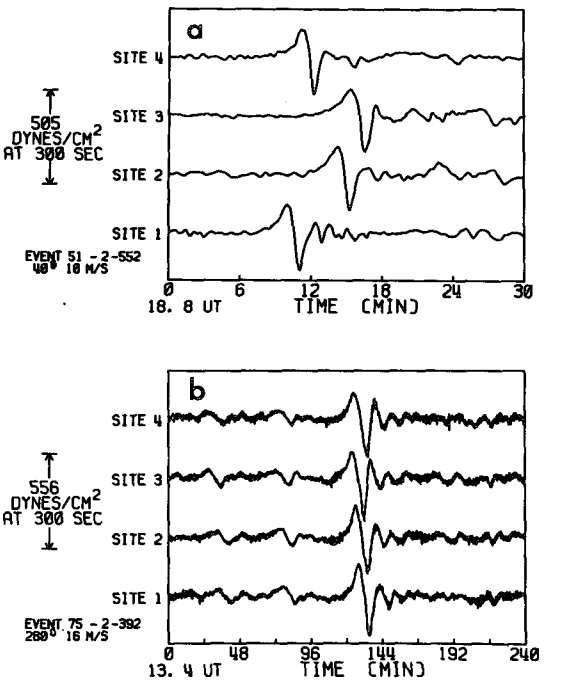

FIG. 8. Microbarometer array record sections which illustrate large-amplitude solitary waves of elevation. Note the almost complete absence of high-frequency components in the micropressure spectrum corresponding to the wake of the wave shown in (a). Two smaller solitary waves precede the unusually large-amplitude event shown in (b).

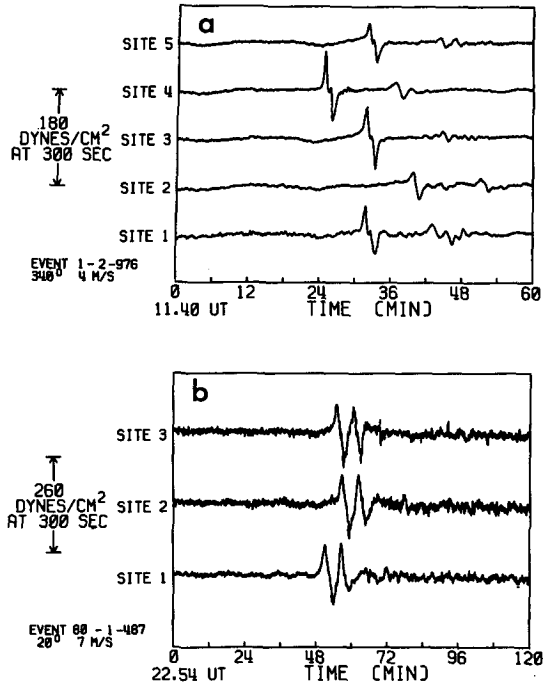

FIG. 9. Examples of unusual solitary wave characteristics for (a) an evolving solitary wave of elevation and (b) a solitary wave group consisting of two closely spaced large-amplitude solitons.

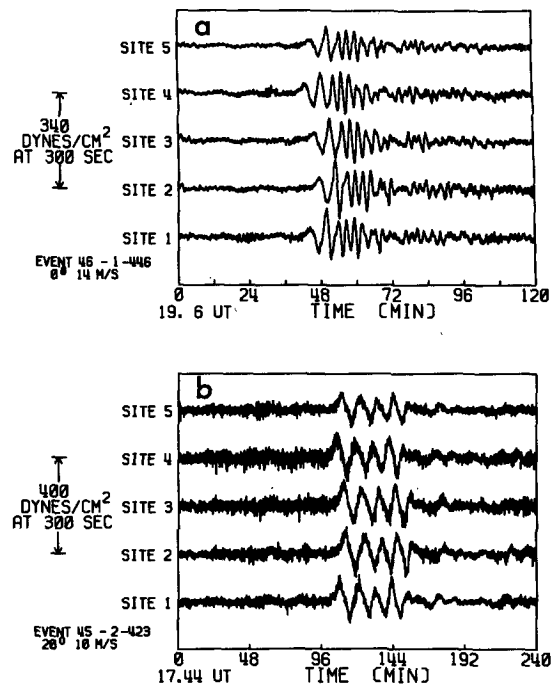

FIG. 11. Two examples of observations of large-amplitude solitary wave packets.

infrasonic array. Almost all of the observed solitary-wave microbarometer signatures correspond to pressure distributions which are similar in form to the theoretical solution profile described by (2.11a). The event shown in Fig. 9a is unusual in that this wave of elevation produced, over part of the observational field, a surface pressure distribution in the form of a broad symmetrical pulse with a relatively flat crest. The significance of this peculiar wave pattern will be considered in more detail in the next section. Groups of waves consisting of well-separated individual solitons are sometimes observed as illustrated in the record sections shown in Fig. 10. In contrast, condensed "wave packets" consisting of two or more closely spaced solitons are frequently observed as shown in the examples in Figs. 9b, 11 and 12. It is worth noting that many of these soliton families are composed of waves of unusually large amplitude. These soliton wave packets may be very complex (see Fig. 12b) but they are usually ordered by amplitude with the higher velocity solitons appearing near the forward edge of the wave packet.

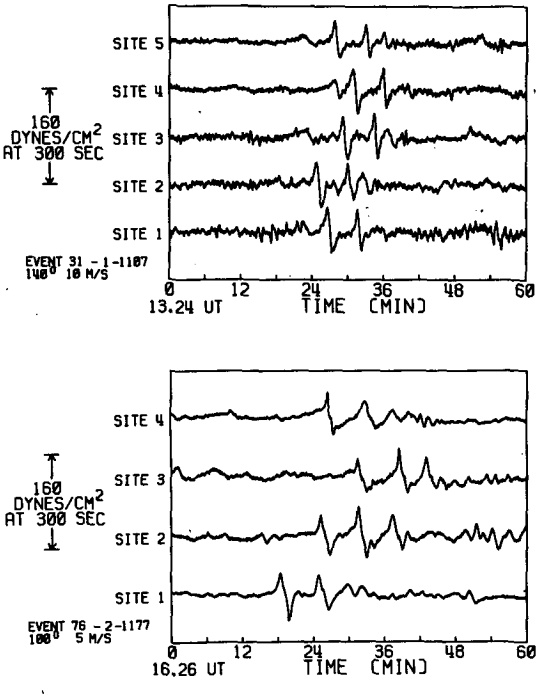

FIG. 10. Infrasonic array record sections containing isolated groups of well-separated solitary waves of elevation.

The salient features of these atmospheric solitary waves have been determined from an examination of the measured properties of 99 events recorded over a two-year period. Waves of this type have been observed with amplitudes as high as 1100 dyn cm^{-2}. They propagate at speeds between 4 and 18 m s^{-1}, with an effective wavelength, as measured by the full width at half maximum, between 0.4 and 7.7 km and tend to occur sometimes for four nights in succession. Note that on a few occasions as many as three of these waves have been observed to pass over the experimental site from different directions within a period of 12 h. Even though the available data span a period of only two years, it seems clear (see Fig. 13) that the frequency of

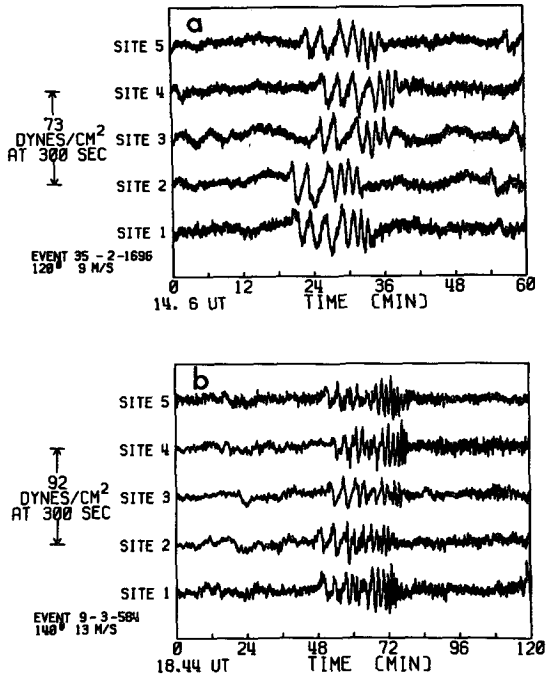

FIG. 12. Record sections which illustrate the signal characteristics of complex low-amplitude solitary-wave packets. In both of these examples the pronounced asymmetry of the differential signal indicates that the wave packet is formed from a family of well-separated solitons.

occurrence of these waves is seasonal. In addition, it appears that waves which generate large-amplitude ($\Delta P > 300$ dyn cm^{-2}) pressure perturbations at the surface occur most frequently from mid-August to mid-October—a period characterized by the formation of intense stable radiation inversions. Contrary to the observations reported by Smart (1966) and Jordan (1972), the waves of elevation observed at Tennant Creek do not occur during the daylight hours between 1000 and 1800 CST (see Fig. 14). A polar plot of the frequency of observation (Fig. 15) reveals that these solitary waves of elevation originate predominatly to

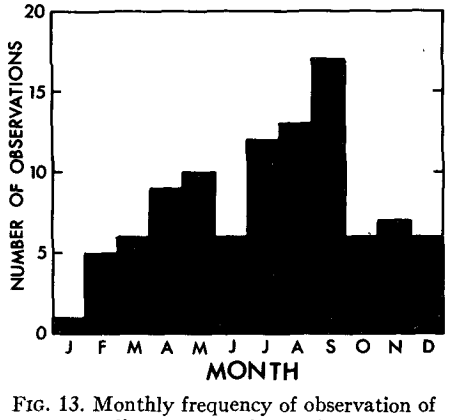

FIG. 13. Monthly frequency of observation of solitary waves of elevation.

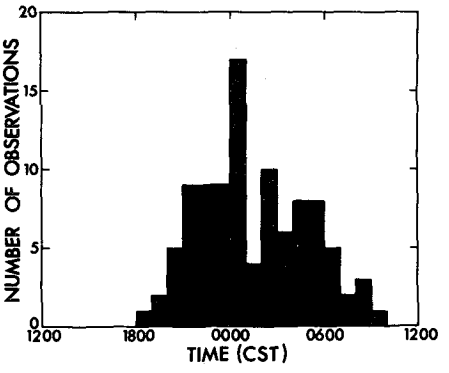

FIG. 14. Frequency of observation of deep fluid solitary waves as a function of time of day.

the north and northeast in the directions of the Timor Sea and the Gulf of Carpentaria and to the southeast in the direction of the Simpson Desert. It is worth remarking on the fact that the majority of the larger amplitude solitary waves of elevation detected at Tennant Creek arrive at the experimental site from azimuths between 20° and 60°.

We now consider the infrasonic array observations of atmospheric solitary waves of depression. In contrast to the high frequency of occurrence of solitary waves of elevation only three waves of depression have been detected during the two-year observational period. An example of an isolated wave of depression may be seen in the microbarograph array record section shown in Fig. 16 for the early morning hours of 30 July 1976. Despite the scarcity of observations it seems clear that these phenomena represent a completely different form of atmospheric solitary-wave disturbance. An examination of the array records indicates that waves of this type propagate with phase velocities between 14 and 50 m s^{-1}, that they have effective wavelengths in the

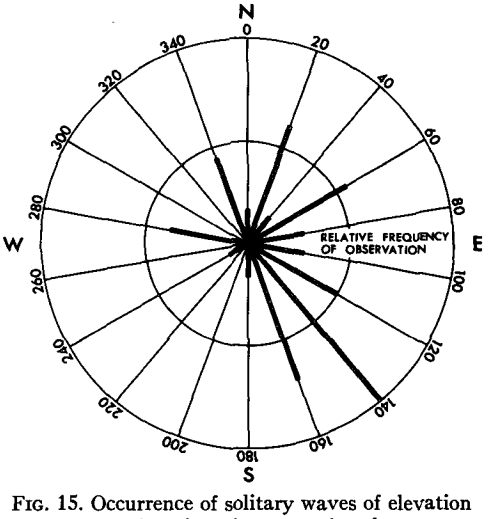

FIG. 15. Occurrence of solitary waves of elevation as a function of source azimuth.

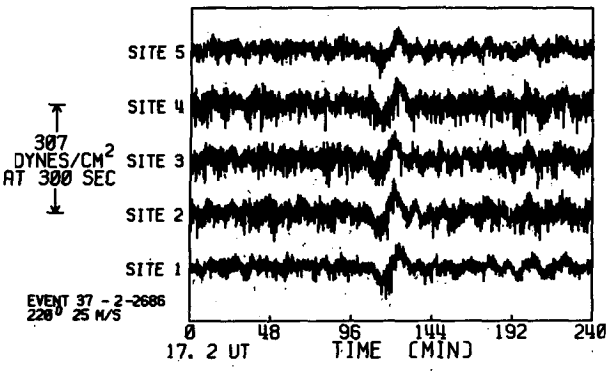

FIG. 16. Microbarograph array observation of a large-amplitude solitary wave of depression.

range from 8 to 30 km, that they produce perturbations in the pressure field at the surface of up to 700 dyn cm^{-2}, and that they originate at an azimuth of 220° as measured from true north. Note that solitary waves of elevation have never been observed to originate in this direction. These properties suggest that the atmospheric scale of this type of isolated disturbance is substantially larger than the scale associated with the deep-fluid solitary waves of elevation. In particular, the unusually high phase velocities indicate that these disturbances are associated with higher altitude atmospheric structure. We therefore tentatively hypothesize that the observed isolated waves of depression properly belong to the classical solitary wave regime, and are in accord with the predictions of the theories of Peters and Stoker (1960), Long (1965) and Benjamin (1966) for classical solitary-wave propagation in a fluid whose density decreases exponentially with height.

In the absence of significant gravity wave activity the micropressure spectrum will be dominated by high-frequency pressure variations produced by turbulent eddies associated with winds near the surface. The influence of this component is evident in the microbarograph array record sections shown in Figs. 7–12 and in Fig. 16. For very low wind conditions, a 6 s acoustic microbarom component is clearly evident, at any time of the year, in the Tennant Creek nocturnal micropressure spectrum. During the day, buoyant convection of unstable turbulent elements created at the surface introduces an additional important component into the micropressure spectrum.

Solitary waves have been observed at Warramunga under a wide variety of meteorological conditions which range from almost totally calm conditions (see Figs. 8a and 10b), indicative of a highly stable boundary layer, through light surface wind conditions with speeds from 1 to 2 m s^{-1} as in the case of the events shown in Figs. 1 and 8b, to higher surface wind conditions with speeds near 4.5 m s^{-1} as in the case of the solitary waves shown in Figs. 11b and 16. The solitary wave propagation vector is not necessarily directed along the surface wind vector. For example, the meteorological measurements show that the surface wind vector and the propagation vectors of the wave packet shown in Fig. 12a and the isolated wave in Fig. 11b differ in azimuth by about 15°, whereas the difference in azimuth for the soliton family in Fig. 11b and the solitary wave of depression shown in Fig. 16 amounts to 90° and 115°, respectively. Note that in all of these cases the passage of the solitary wave appears to have had no lasting influence on the surface wind. It is also worth noting that solitary waves have been observed during periods of local thunderstorm activity and also under totally clear conditions where storm activity is completely absent within 500 km of the array.

Perhaps the most significant meteorological observation is the fact that the surface temperature and humidity are not perturbed by the passage of isolated solitary waves and isolated soliton wave packets. An example which illustrates the observations of surface wind speed, wind direction, temperature and humidity during the passage of a solitary wave of elevation is given in Fig. 17. This particular event was chosen for illustration since it is well defined (see Fig. 1) and since it occurred during a period of fairly quiet atmospheric conditions near the surface. As can be seen from the diagram, the wind vector is virtually unchanged by the passage of the wave and no measurable perturbation in either the temperature or humidity can be associated with the main body of the wave or with the region in the wake of the wave. The dynamical properties of the atmosphere in the wake of the wave therefore appear to be almost

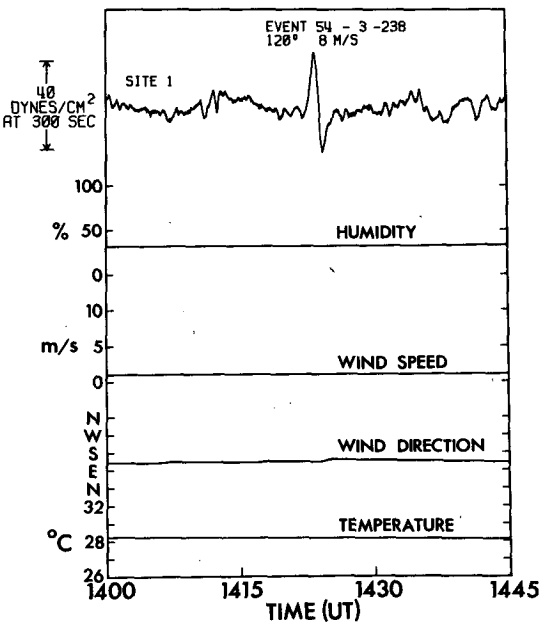

FIG. 17. Microbarograph record and corresponding measurements of surface temperature, humidity, wind speed and wind direction, recorded at site 1, for the solitary wave of elevation which passed over the infrasonic array at 23.53 on the night of 2 December 1976.

the same as the conditions which prevailed prior to the arrival of the solitary wave.

5. Discussion and conclusions

A detailed comparison of the observed properties of atmospheric solitons with the predictions of solitary-wave theory is complicated by the fact that the theoretical treatments have been restricted to static models with simple forms of the vertical density profile. Perhaps the most serious criticisms of the direct application of these models to nonlinear wave propagation in the earth's atmosphere are the neglect of wind shear (within the limits of dynamic stability) and the oversimplification of the fluid density structure.

In the discussion of the static theories it was noted that the classical solitary wave of elevation is stable to an amplitude of 0.827. The stability limits for other types of classical waves, such as the solitary wave of depression, and for all forms of deep-fluid solitary wave are unknown; it is, however, clear from the work of Davis and Acrivos (1967) that the limits for deep-fluid solitary waves extend to much larger amplitudes. The fact that solitary waves can exist with very large amplitudes raises the possibility that waves of this type may significantly alter the dynamical properties of the atmosphere. This interaction could result from a tendency of very large-amplitude waves to break[2]—this complicated process can occur in either the forward or backward direction according to the specific form of the wind and density profiles (Long, 1956a, 1972)—or from a process of turbulent entrainment of fluid near the crest into the circulation pattern associated with the wave thus leading to turbulence in the wake and to further long-period oscillations corresponding to the motion of displaced buoyant fluid elements. A description of a rare observation of an evolving wave of elevation which may represent a breaking internal solitary wave is given below. If the atmospheric solitary waves described here possess an intrinsic turbulent wake then they are losing energy rapidly and it must be expected that they are of limited range.

Consider now the implications of the laboratory observations and numerical calculations of Davis and Acrivos (1967) on solitary waves propagating in a thin layer of fluid contained between two deep fluids comprising a stably stratified system. As has already been noted, these authors found that waves of large amplitude develop closed streamlines characteristic of the circulation in a vortex pair and, further, that these waves shed semi-periodic waves behind the main disturbance. It follows directly from an argument based on dynamic symmetry (Benjamin, 1967) that a single vortex occurs within large-amplitude solitary waves associated with an inhomogeneous shallow layer of fluid lying beneath a much deeper homogeneous fluid and that this internal circulation coupled with the entrainment hypothesis could lead to the development of a turbulent wake.

A measure of the influence of solitary wave propagation on the dynamical properties of the atmosphere is provided by a comparison (Fig. 18) of the power spectral densities of the surface pressure field evaluated before and after the passage of the wave. Since this technique includes contributions from fluid motions at high altitudes it should be particularly sensitive to changes in the atmosphere flow field induced by the main body of the wave—changes which may not be apparent in the observations of the flow field at the surface. An examination of all of the cases illustrated in Fig. 18 shows that the spectral character of the atmosphere is largely unaffected by the passage of the wave. In particular, the power spectra shown in Figs. 18a and 18b for a solitary wave of elevation and in Fig. 18d for a solitary wave of depression indicate that the spectral characteristics both before and after the passage of the event are identical. In the case of the event shown in Fig. 18c, the wave of elevation appears to be associated with a slight increase in the amplitude of longer period spectral components. It is worth noting that in all of the three examples illustrated for solitary waves of elevation an identical 4–6 s peak due to microbarom activity appears prominently in both the spectrum evaluated ahead of the wave and the spectrum evaluated after the passage of the wave. The slight increase in the amplitude of the longer period components in the wake of the event in Fig. 18c—if at all significant—may be a measure of the irregular waves described by Davis and Acrivos (1967) which are shed by large-amplitude deep-fluid solitary waves or it may merely represent a small-amplitude component of the original disturbance which gave rise to the solitary wave.

The fact that an additional high-frequency component is absent in the micropressure spectrum corresponding to the wake of these waves suggests that these isolated solitons do not induce turbulence into the atmosphere. The results of this analysis coupled with the observation of an undisturbed surface flow field therefore leads to the conclusion that these disturbances do not significantly perturb the dynamical state of the atmosphere and that they represent essentially pure solitary-wave motion.

Solitary waves are normally observed to pass over the experimental site as highly coherent stationary linear wave fronts. The example illustrated in Fig. 9a is exceptional in that this particular wave of elevation was observed to evolve substantially over the 4 km

[2] The term "wave-breaking" is used here in the general sense of Long (1972) to denote any tendency for the isolated wave to steepen behind or ahead of the crest as it propagates. If this proves to be the case for large-amplitude atmospheric solitons then the dynamics of these waves may well be dominated by amplitude dispersion and they must therefore be viewed as quasi-stationary phenomena.

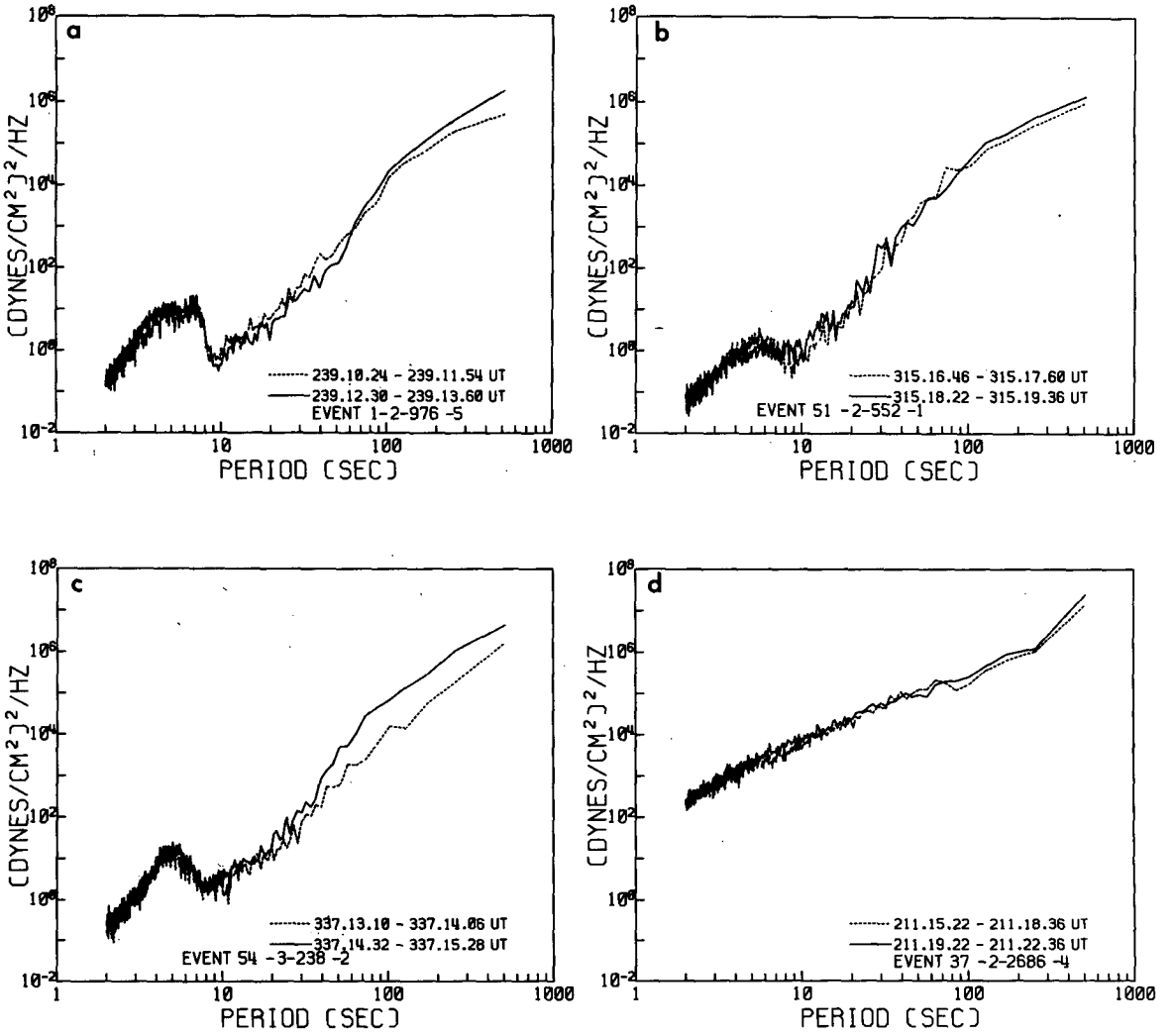

FIG. 18. Some comparisons of the micropressure power spectral density ahead of and in the wake of isolated waves which illustrate the influence of the passage of internal solitary waves on the atmospheric spectrum. High-frequency changes in the spectral estimates may be viewed as a measure of the degree of solitary wave-induced atmospheric turbulence. The analyses in (a), (b) and (c) correspond to solitary waves of elevation; the spectra shown in (d) correspond to a solitary wave of depression.

aperture of the infrasonic array. This is the only example of an evolving solution wave pattern to be observed during the two-year experimental period. The degree of evolution may be seen in the detailed diagrams presented in Fig. 19 which show both the microbarogram recordings at each array site and the corresponding true surface pressure variation as determined from the measured data through an inversion of the instrumental response specified by (3.1). This wave of elevation first appeared at site 4 and was then observed to propagate along the diagonal of the quadrilateral array to site 2. The evolution of the solitary wave can therefore be followed by examining the sequence of wave patterns at sites 4, 5 and 2. As can be seen from the figure, the isolated wave steadily decreases in amplitude over the array and evolves from the unusual symmetric profile with a flattened crest observed at site 4 to the familiar deep-fluid Lorentz soliton profile observed at site 2. This pattern of evolution is further reflected in a steady decrease in the phase velocity from about 4.7 m s^{-1} to 4.2 m s^{-1}.

There are a number of possible interpretations of this unusual evolving wave pattern. For example, as has already been noted, the form of the pressure distribution in the neighborhood of the crest of the initially observed wave could indicate an amplitude instability leading to a type of internal wave breaking which might be manifested in the production of turbulence at the crest through the Kelvin-Helmholtz mechanism. However, our current preferred explanation of this evolving wave pattern is that it represents the transition observed in the laboratory by Davis and Acrivos (1967)

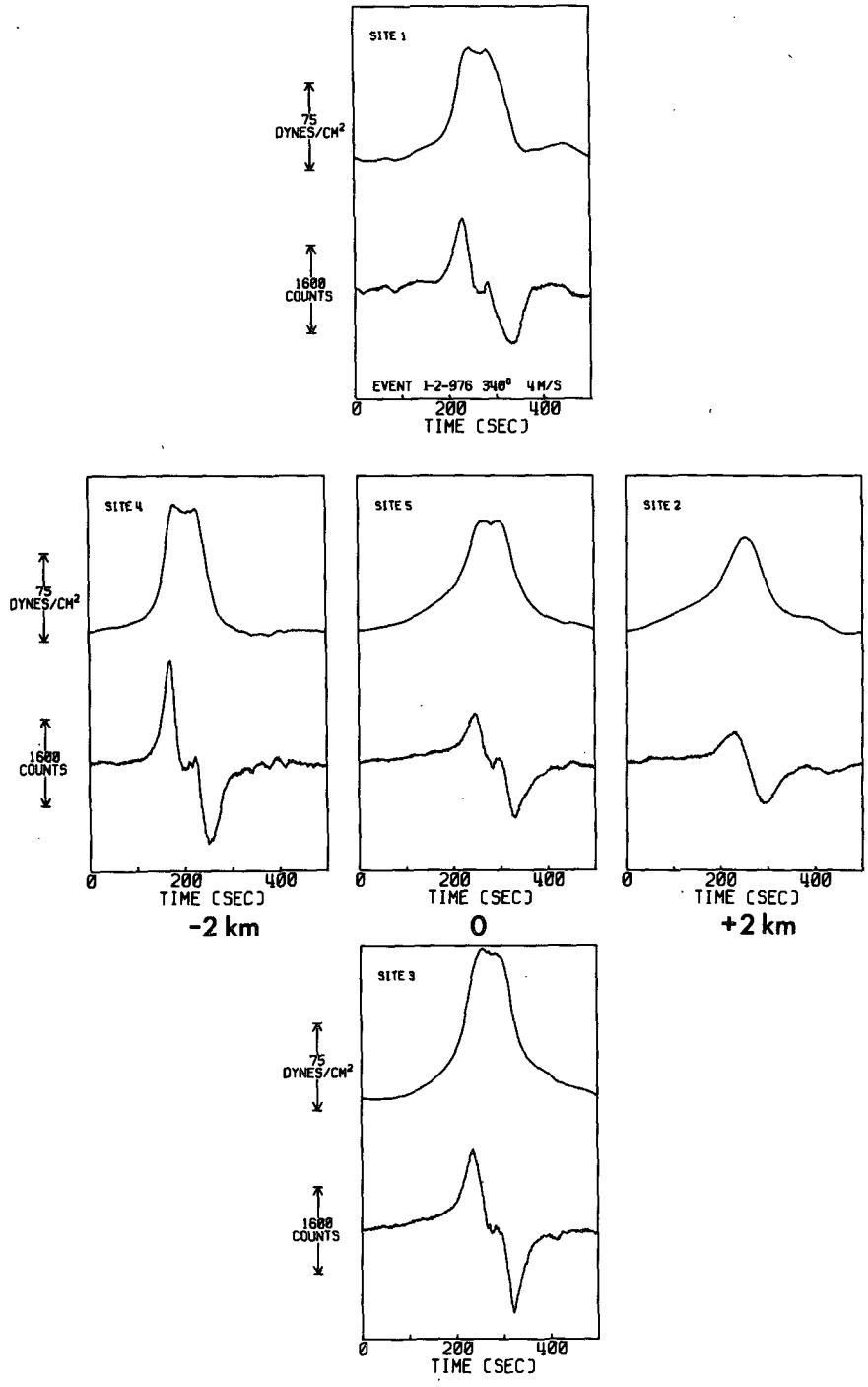

FIG. 19. Surface pressure characteristics produced by an unusual evolving solitary wave of elevation. Both the recorded microbarograph solitary wave signature (lower trace) and the derived absolute surface pressure perturbation (upper trace) are shown in detail for each site of the intrasonic array.

of a large-amplitude deep-fluid solitary wave with closed internal circulation to a smaller amplitude wave with an open streamline flow pattern characteristic of pure wave motion. It is evident that a complete understanding of the dynamical structure of these waves will require further extensive experimental observations of evolving soliton wave patterns.

We now consider some estimates of the intensity ΔT and height h of the nocturnal inversion and a measure of the dimensionless solitary-wave amplitude α which

TABLE 1. Measured properties of internal solitary atmospheric waves of elevation and corresponding theoretical estimates of the intensity and height of the temperature inversion and of the solitary-wave amplitude based on Benjamin's first-order approximation to the two-component deep-fluid solitary-wave solution. The measured signal amplitude and full width of the profile at half maximum are obtained from array averages corrected for instrumental response.

Event	Day	Time (CST)	Velocity c (m s^{-1})	Azimuth θ (deg)	Signal amplitude ΔP (dyn cm^{-2})	Full width at half maximum $w_{\frac{1}{2}}$ (km)	Inversion intensity ΔT (°C)	Inversion height h (m)	Solitary wave amplitude $\alpha=a/h$
63-1-1233*	34	0216	4	20	50	0.47	6.8	55	0.32
76-2-1177*	140	0228	5	100	50	0.51	12.2	42	0.23
1-2-976	238	2146	4	340	80	0.39	3.6	88	0.61
80-1-487*	167	0920	7	20	300	1.30	2.2	390	0.83
51-2-1318*	315	0524	13	280	450	4.40	9.2	430	0.27
75-2-392	133	2258	16	280	1100	7.70	3.8	1400	0.49

* Leading soliton in solitary wave group.

may be obtained to a first approximation from measurements of the surface pressure perturbation ΔP, the effective wavelength $w_{\frac{1}{2}}$ and the wave speed c by applying Benjamin's two-fluid solitary wave solution (2.11) to the lower atmosphere. To this approximation

$$\alpha=\frac{\Delta P}{\rho_1 c^2-\frac{3}{4}\Delta P}, \tag{5.1}$$

$$\Delta T=\tfrac{1}{2}T[1-(1-\delta)^{\frac{1}{2}}], \tag{5.2}$$

$$h=\beta\left(1-\frac{\Delta T}{T}\right), \tag{5.3}$$

where

$$\beta=\tfrac{3}{8}\alpha w_{\frac{1}{2}}, \quad \delta=4\Delta P/g\beta\rho_1\alpha,$$

T is the temperature of the upper fluid and ρ_1 the density of the lower fluid. In these expressions, the intensity of the inversion and the height of the inversion above the surface are to be regarded as the effective parameters of a two-layer model which provides the simplest possible description of the complex thermal structure of the nocturnal inversion. In these calculations, T is taken as 280 K and the lower fluid density is held constant at 1.2×10^{-3} g cm^{-3} corresponding to an inversion near the 980 mb level. The results are presented in Table 1.

The events listed in this table were chosen to illustrate the properties of a wide variety of isolated solitary wave forms. All of these events occurred under low surface wind conditions. It should be noted that the derived parameters corresponding to waves of large amplitude may be unreliable since the theory is valid only to first order in α. As can be seen from the table, this model indicates that solitary-wave activity is usually associated with a temperature inversion with an effective depth between 40 to 400 m and with an effective intensity in the range from about 2 to 12°C. The first entries in the table describe solitary-wave propagation along a relatively shallow inversion; these events are typical of many of the low-amplitude solitary-wave signals which have been observed.

There are, as yet, no suitable measurements of the nocturnal inversion temperature profile with which these results can be compared. Clarke *et al.* (1971) have reported the results of atmospheric soundings at Hay, N.S.W., 2000 km to the southeast of Tennant Creek, which reveal nocturnal inversion depths from 80 to 200 m and intensities of up to about 5°C. It can be expected that the lower latitude location and semi-desert environment of the Tennant Creek infrasonic array will favor the development of much stronger nocturnal radiation inversions. This is in agreement with inversion intensities of up to 10°C observed by Reynolds and Gething (1970) at Julia Creek during the course of their acoustic sounding experiments. It therefore seems reasonable to conclude that almost all of the isolated waves of elevation detected at Warramunga are deep-fluid solitary waves which propagate along a nocturnally cooled surface layer.

The very large-amplitude event which occurred on day 392 is exceptional in that the scale associated with this particular solitary wave is significantly greater than that of any other wave of elevation detected during the two-year observational period. It is therefore suggested, in view of the atmospheric scale involved, that this particular wave may be better described as a classical solitary wave of elevation which is similar, although on a smaller scale, to the solitary-wave disturbance reported by Abdullah (1955).

It must be emphasized at this point that any discussion of the source mechanisms which excite these solitary waves is largely conjectural since the range and lateral extent of these waves are almost totally unknown. Existing evidence, such as the fact that these waves traverse the 4 km infrasonic array as highly coherent planar wave-fronts and the observation, noted above, by Reynolds and Gething (1970) that solitary wave associated disturbances appear to propagate essentially unattenuated over distances of about 40 km,

suggests that these waves originate at large distances from the array. However, if the internal morphology of the waves takes the form of a closed circulation leads to an intrinsic tendency to shed semi-periodic disturbances behind the main body or if these waves are breaking, then they are rapidly losing energy and it must therefore be anticipated that they are of limited range. On the other hand, the experimental observations do not indicate the presence of significant wave-induced turbulence; it therefore appears that the waves of elevation could have a range of up to about 600 km, the limit set by the speed of the wave and the duration of the nocturnal inversion.

Perhaps the first question that should be considered is whether or not the solitary waves observed near Tennant Creek are due to the passage of a frontal system. Dry, cold fronts occur with reasonable frequency over the extreme southern portion of Australia. These fronts seldom reach the center of the continent and are very rare at the experimental site in the Northern Territory. An examination of the isochrones of these cold fronts shows that the few degenerate fronts which extend to Tennant Creek arrive from an azimuth near 220°. It has been established that solitary waves of elevation originate predominantly in directions near 20° and 140°, that they never originate in the direction of 220°, that they only occur at night, that they often occur on several nights in succession and that two or more of these waves may pass over the experimental site from different directions during the same night. All of these observations are inconsistent with an interpretation involving the passage of a cold front. In addition, the microbarograph records of these well-defined isolated waves of elevation bear little resemblance to the complex micropressure pattern recorded by McDonald (1974) during the passage of a frontal system over an array located in northern Texas. It therefore seems very unlikely that cold fronts play an important role in the production of deep-fluid atmospheric solitons.

In contrast, the three classical solitary waves of depression detected at Tennant Creek do appear to originate in the same direction as atmospheric fronts. However, an examination of the synoptic patterns fails to confirm that these events coincided with the passage of a cold frontal system; nevertheless, the possibility that these large-amplitude waves occur in conjunction with weak frontal activity should not be ruled out at this point.

Smart (1966) and Jordan (1972) associate their observed exponential pressure pulses with thunderstorms. The organized, precipitation-initiated and precipitation-maintained downdraft of cold air in severe mature storms is well documented (Wallington, 1961; Browning and Ludlam, 1962; Spillane and McCarthy, 1969). Smart developed a model to describe these pressure pulses by considering the unstable solution of Brunt's well-known basic equation of motion (Brunt, 1927) for the vertical displacement (dh) of a parcel of air[3]

$$\frac{d^2(dh)}{dt^2}+\frac{g}{T}\left(\beta+\frac{dT}{dh}\right)dh=0. \tag{5.4}$$

Brunt noted that if the lapse rate $-dT/dh$ is greater than the adiabatic lapse rate β, no restoring force exists and consequently a downward displaced air parcel will continue to accelerate exponentially. Smart adapted this result to explain the observed form of the pressure pulses by noting that the downward descending parcel is subject to a constant pressure gradient and thus the density of the parcel increases exponentially with the result that (assuming the approximate validity of the hydrostatic law) the ground-level pressure contains an exponentially increasing component. Smart also hypothesized that the downward motion continues to accelerate in smooth laminar flow until a critical velocity is reached, at which point the flow becomes turbulent and mixes rapidly with nearby warmer air thus causing rapid oscillations behind the pulse and, eventually, a reduction of the pressure to the ambient level. On the basis of this model, Smart was able to account for 4 out of 10 observations of exponential pressure pulses.

There appear to be a number of difficulties associated with this model, the most serious of which is the fact that this explanation is applicable only to observations recorded directly beneath a thunderstorm downdraft; it must be expected that the ground-level pressure distribution outside this very localized region is of a completely different form. Consequently, the observations reported by Jordan (1972) of pressure pulses coming from thunderstorms at distances of the order of 100 km are not accounted for by this model as it stands.

It is an obvious extension of this model to include the influence of the gravity current of undercutting cold air that advances away from the thunderstorm as the downdraft spreads out at the surface. Wallington (1961) noted an example in which this density current extended over 50 km and the subject has recently been treated in detail by Charba (1974) and by Goff (1976). An interesting description of a Sudanese *haboob*, a downdraft gravity current made visible by its high dust content, has been given by Lawson (1971). A reasonable explanation of long-range thunderstorm-generated pressure pulses is that they represent solitary waves produced by either the direct impulsive interaction of the

[3] Priestley (1953) has derived simultaneous equations which describe the vertical motion and temperature of buoyant fluid elements subject to turbulent mixing with the surroundings. A more general theoretical treatment which includes the effect of turbulent fluid entrainment has been given by Turner (1963). In the case of unstable environments solutions exist for both of these models in which the velocity of the fluid element ultimately increases exponentially with time. These models provide a firmer basis for a description of downdraft flow in thunderstorms.

downdraft on an inversion or the concommitant interaction of the gravity current with an existing inversion. The latter mechanism is closely related to the phenomenon of soliton production in the developing frontal zone of an advancing bore as shown in the numerical studies of Peregrine (1966) and Vleigenthart (1971) on the evolution of nonstationary solutions of the KdV equation.

According to the comprehensive study of Goff (1976), the abrupt transition in surface atmospheric conditions which accompanies the passage of the frontal zone of a well-developed quasi-steady downdraft-produced density current is characterized by a sharp decrease in temperature in the range from 2 to 10°C, a sudden onset of persistent winds and a rapid increase of about 3.4 mb on the average in the surface pressure level. This transition is usually followed by the onset of precipitation. It is clear that a downdraft gravity current interpretation fails to account for the isolated nocturnal disturbances described in this paper since none of these perturbations of the atmospheric flow field are observed (see Fig. 17) to accompany these events.

It is possible that some of the solitary waves observed at Tennant Creek during the monsoon season from December to February are due to thunderstorm activity. Note, however, that only one solitary wave has been observed during the month of January. As can be seen from the monthly frequency analysis shown in Fig. 13, solitary waves are most commonly observed during the period from April to September, a period of very low storm activity. Furthermore, solitary waves have been observed to occur under completely clear conditions when storm activity is absent within several hundred kilometers of the array. We therefore conclude that the thunderstorm source mechanism is of minor importance.

The fact that solitary waves of elevation come from preferred directions suggest that they may be orographic in origin. First we note the large number of observations of isolated waves which arrive from an azimuth of 140°. These waves are usually detected near midnight but they also occur with reasonable frequency at other times during the night. As one proceeds in the direction of 140° from the infrasonic array the terrain can be described, initially, as a more or less flat featureless plain. At about 10 km from the array a complicated pattern of hills comprising the Murchison Range begins to appear on the right at a distance of about 5 km. This chain of hills, which rises to a maximum elevation of about 200 m over the surrounding plain, runs parallel to the 140° direction for a distance of about 100 km. Beyond this point the level plain slowly gives way to the Davenport Range which intersects the Murchison Range at the same altitude at about 140 km from the array. Further afield in this direction, the terrain descends to an arid plain which continues uninterrupted and finally merges with the Simpson Desert at a distance of about 460 km.

The presence of these nearby ranges suggests that the origin of solitary waves coming from this direction is to be found in the interaction with an existing inversion of katabatic (downslope) nocturnal flow of surface-cooled air from these hills onto the surrounding plain. The hypothesis of supercritical katabatic drainage leading to an internal atmospheric hydraulic jump has been employed with considerable success by Ball (1965; see also Ball, 1957; Lied, 1964) to explain the sudden stationary discontinuity found in surface winds in the Antarctic. Similarly, Clarke (1972) has explained a frequently occurring, sudden, near-dawn squall, accompanied by a spectacular low horizontal roll cloud known as the "morning glory", on the south coast of the Gulf of Carpentaria by evoking the concept of a propagating undular gravity current created in the process of nocturnal surface flow down a 1:1000 slope from the 500 m highlands to the east. Clarke carried out a number of numerical experiments and concluded that internal atmospheric bores and propagating hydraulic jumps should commonly occur at low latitudes when katabatic flow discharges onto a plain under conditions of a stable radiation inversion.

This conclusion appears to be reinforced by the acoustic soundings at Julia Creek reported by Reynolds and Gething (1970) which revealed, as has already been noted, the occurrence of a jump in the height of the nocturnal inversions. These authors also hypothesized the existence of katabatic flow aided in part by the geostrophic wind and orographic convergence and concluded that the observed jumps in the inversion level could be attributed to either the head of a gravity current propagating as an internal bore or a traveling internal hydraulic jump.

Since the rise in topography in this direction appears to be sufficient to produce significant nocturnal boundary layer currents, it is proposed that the observed solitary waves coming from an azimuth of 140° are generated in the interaction of katabatic flow with the nocturnal inversion and that they propagate along the inversion to the array. It is premature, without further experimental work, to examine this mechanism in detail but it probably takes one of the following forms:

1) The direct impulsive interaction of an advancing gravity current impinging on an established inversion.

2) The disturbance of the atmospheric flow field during the creation (or dissipation) of a hydraulic jump; this may occur at the point where supercritical downslope flow encounters the horizontal plane—this hydraulic jump may subsequently propagate upstream or downstream as flow conditions vary—or in conjunction with a supercritical-subcritical flow transition in the neighborhood of a topographic barrier on the horizontal plane.

3) The momentary transition of a steady advancing bore to a nonstationary flow state upon encountering a topographic obstacle such as a ridge or valley.

4) The direct soliton production in the evolving frontal zone of a gravity current as described above for downdraft-associated density currents, probably the most important mechanism.

The interpretation in terms of katabatic flow at an orographic feature accounts for both the occurrence of waves coming from the direction of 140° and for the scarcity of events originating in the southwest quadrant where orographic features suitable for the production of katabatic flow are absent. However, an attempt to apply an interactive katabatic wind interpretation to account for the source of the large number of solitary waves which originate in the northeast and northwest quadrants is less successful. Thus for waves which arrive from the direction of the Gulf of Carpentaria, the elevation decreases steadily from about 410 m MSL to 200 m at a distance of about 150 km from the array. From this point, the land rises slowly to form the Barkly Tablelands at an altitude of about 260 m. At the edge of the Tablelands, about 340 km from the array, the land again rises to about 310 m and then falls continuously to the hot tropical coast of the Gulf 500 km from the array.

It is possible that solitary waves originating in this direction are produced in the dissipation of gravity currents flowing toward the array into the broad shallow valley which separates Warramunga and the Barkly Tablelands. However, in this case the topography would not appear to support significant katabatic flow. A katabatic density current interpretation for the source of events originating to the east and northeast can be ruled out for the same reason. A different type of source mechanism is therefore required to explain the solitary waves which originate in these directions.

An indication of the range of isolated waves which originate to the north of the array is given by the observation that the majority of these events are observed to occur between 0200 and 0700 CST. This suggests that the source of these waves is to be found at a considerable distance from the array. If it is assumed that these waves are created during or shortly after the formation of a stable inversion then the average measured speed of 10 m s^{-1} is consistent with a source in the neighborhood of the coastal edge of the Barkly Tablelands. This suggests that the solitary waves observed at Warramunga which originate in the directions of the Gulf of Carpentaria and the Timor Sea may represent the final form of deeply penetrating sea-breeze fronts. Solitary-wave production might proceed, as described above, through the formation of a solution wave packet along the leading edge of a shallow sea-breeze current or simply through the evolution of the direct density current produced disturbance of the inversion layer. Insight into the nature of a new and probably more important mechanism is provided by the recent observations described by Simpson *et al.* (1977) of the formation of a horizontal vortex at the head of a sea-breeze front which separates from the sea breeze shortly before sunset and continues to propagate as an independent phenomenon. The unusual stability of a propagating semi-elliptical horizontal atmospheric vortex has been considered by Clarke (1965). Since closed circulation in the form of a propagating vortex is also a characteristic of large-amplitude deep-fluid solitary waves, it is reasonable to assume that a sea-breeze generated vortex which interacts with the nocturnal inversion will eventually evolve into an internal atmospheric solitary wave.

This concludes the description and interpretation of atmospheric internal solitary waves which are observed in the arid interior of Australia. It is evident that further measurements of the properties of these waves are required if a full understanding of phenomena of this type is to be achieved. In particular, the evolution of the frontal zone of a shallow internal density current advancing into a deep stratified fluid and the role played by disturbances of this type in the production of solitary waves deserve further study. The experimental program at Warramunga is therefore being expanded to include further meteorological instrumentation. In addition, the infrasonic array is being enlarged, through the addition of portable array elements, to an aperture of about 100 km. With the completion of this program it should be possible to carry out a detailed investigation of the degree of wave coherence over large distances and to establish with certainty the source mechanisms responsible for the creation of waves of this type.

Acknowledgments. The authors wish to express their gratitude to Professor J. S. Turner for helpful comments on a first draft of this paper and to Dr. J. F. Gettrust for several stimulating discussions during the course of this research. We thank also an unknown reviewer for comments on an earlier draft of this paper. These comments have led to the inclusion of some data from more recent observations at Tennant Creek. In addition, we wish to thank Mr. David Daffen and Mr. Blair Lade for their efforts in operating and maintaining the Warramunga Seismic Station. This research was supported by the Air Force Office of Scientific Research under Contract AFOSR 75.2759A.

REFERENCES

Abdullah, A. J., 1949: Cyclogenesis by a purely mechanical process. *J. Meteor.*, **6**, 86–97.

——, 1955: The atmospheric solitary wave. *Bull. Amer. Meteor. Soc.*, **36**, 515–518.

——, 1956: A note on the atmospheric solitary wave. *J. Meteor.*, **13**, 381–387.

Ball, F. K., 1956: The theory of strong katabatic winds. *Aust. J. Phys.*, **9**, 373–386.

——, 1957: The katabatic winds of Adélie Land and King George V Land. *Tellus*, **9**, 201–208.

Benjamin, T. B., 1966: Internal waves of finite amplitude and permanent form. *J. Fluid Mech.*, **25**, 241–270.

——, 1967: Internal waves of permanent form in fluids of great depth. *J. Fluid Mech.*, **29**, 559–592.

Bingham, C., M. D. Godfrey and J. W. Tukey, 1967: Modern techniques of power spectrum estimation. *Trans. IEEE*, **AU-15**, No. 2, 56–66.

Boussinesq, J., 1871: Théorie de l'intumescence liquide appelée onde solitaire ou de translation se propageant dans un canal rectangulaire. *Inst. France Acad. Sci. C. R.*, June 19, p. 755.

Browning, K. A., and F. H. Ludlam, 1962: Airflow in convective storms. *Quart. J. Roy. Meteor. Soc.*, **88**, 117–135.

Brunt, D., 1927: The period of simple vertical oscillations in the atmosphere. *Quart. J. Roy. Meteor. Soc.*, **54**, 30–32.

Byatt-Smith, J. G. B., 1970: An exact integral equation for steady surface waves. *Proc. Roy. Soc. London*, **A315**, 405–418.

——, and M. S. Longuet-Higgins, 1976: On the speed and profile of steep solitary waves. *Proc. Roy. Soc. London*, **A350**, 175–189.

Chan, R. K.-C., 1974: A discretized solution for the solitary wave. *J. Comput. Phys.*, **16**, 32–48.

Charba, J. 1974: Application of gravity current model to analysis of squall-line gust front. *Mon. Wea. Rev.*, **102**, 140–155.

Clarke, R. H. 1965: Horizontal mesoscale vortices in the atmosphere. *Aust. Meteor. Mag.*, **50**, 1–25.

——, 1972: The morning glory: an atmospheric hydraulic jump. *J. Appl. Meteor.*, **11**, 304–311.

——, A. J. Dyer, R. R. Brook, D. G. Reid, and A. J. Troup, 1971: The Wangara experiment: Boundary layer data. Tech. Pap. No. 19, Division of Meteor. Physics, CSIRO.

Davis, R. E., and A. Acrivos, 1967: Solitary internal waves in deep water. *J. Fluid Mech.*, **29**, 593–607.

Fenton, J., 1972: A ninth-order solution for the solitary wave. *J. Fluid Mech.*, **53**, 257–271.

Friedrich, K. O., 1948: On the derivation of the shallow water theory. Appendix to J. J. Stoker, The formation of breakers and bores. *Comm. Pure Appl. Math.*, **1**, 81–87.

——, and D. H. Hyers, 1954: The existence of solitary waves. *Comm. Pure Appl. Math.*, **7**, 517–550.

Goff, R. C., 1976: Vertical structure of thunderstorm outflows. *Mon. Wea. Rev.*, **104**, 1429–1440.

Gossard, E. E., and W. H. Hooke, 1975: *Waves in the Atmosphere.* Elsevier, 456 pp.

Grimshaw, R., 1971: The solitary wave in water of variable depth. Part 2. *J. Fluid Mech.*, **46**, 611–622.

Hurdis, D. A., and H. Pao, 1975: Experimental observation of internal solitary waves in a stratified fluid. *Phys. Fluids*, **18**, 385–386.

Jordan, A. R., 1972: Atmospheric gravity waves from winds and storms. *J. Atmos. Sci.*, **29**, 445–456.

Kanasewich, C. D., C. D. Hemmings and T. Alpaslan, 1973: *N*-th root stack nonlinear multichannel filter. *Geophysics*, **38**, 327–338.

Karpman, V. I., 1975: *Non-linear Wind Dispersive Media.* Pergamon Press, [Trans. from Russian].

Keller, J. B., 1948: The solitary wave and periodic waves in shallow water. *Comm. Pure Appl. Math.*, **1**, 323–339.

Keulegan, G. H., 1953: Characteristics of internal solitary waves. *J. Res. Nat. Bur. Stnd.*, **51**, 133–140.

Korteweg, D. J., and G. de Vries, 1895: On the change of form of long waves advancing in a rectantular canal and on a new type of long stationary waves. *Phil. Mag.*, **39**, 422–443.

Laitone, E. V., 1960: The second approximation to cnoidal and solitary waves. *J. Fluid Mech.*, **9**, 430–444.

Lamb, H., 1932: *Hydrodynamics*, 6th ed. Cambridge University Press, 423–426.

Lavrent'ev, M. A., 1947: On the theory of long waves. *Akad. Nauk. Ukrain. RSR., Zbornik Prac. Inst. Mat.*, 1946, No. 8, 13–69. [Trans. in *Amer. Math. Soc. Transl.*, Ser. 1, **11**, 273–321, 1962].

Lawson, T. J., 1971: Haboob structure at Khartoum. *Weather*, **26**, 105–112.

Lenau, C. W., 1966: The solitary wave of maximum amplitude. *J. Fluid Mech.*, **26**, 309–320.

Lied, N. T., 1964: Stationary hydraulic jumps in a katabatic flow near Davis, Antarctica, 1961. *Aust. Meteor. Mag.*, **47**, 40–51.

Long, R. L., 1956a: Long waves in a two-fluid system. *J. Meteor.*, **13**, 70–74.

——, 1956b: Solitary waves in one- and two-fluid systems. *Tellus*, **8**, 460–471.

——, 1965: On the Boussinesq approximation and its role in the theory of internal waves. *Tellus*, **17**, 46–52.

——, 1972: The steepening of long, internal waves. *Tellus*, **24**, 88–99.

Longuet-Higgins, M. S., and J. D. Fenton, 1974: On the mass, momentum energy and circulation of a solitary wave. II. *Proc. Roy. Soc. London*, **A340**, 471–493.

McAllister, L. G., J. R. Pollard, A. R. Mahoney and P. J. R. Shaw, 1969: Acoustic sounding—a new approach to the study of atmospheric structure. *Proc. IEEE*, **57**, 579–587.

McDonald, J. A., 1974: Naturally occurring atmospheric acoustical signals. *J. Acoust. Soc. Amer.*, **56**, 338–351.

Muirhead, K. J., 1968: Eliminating false alarms when detecting seismic events automatically. *Nature*, **186**, 704.

——, and Datt Ram, 1976: The *N*th root process applied to seismic array data. *Geophys. J. Roy. Astron. Soc.*, **47**, 197–210.

Peregrine, D. H., 1966: Calculations of the development of an undular bore. *J. Fluid Mech.*, **25**, 321–330.

Peters, A. S. and J. J. Stoker, 1960: Solitary waves in liquids having non-constant density. *Comm. Pure Appl. Math.*, **13**, 115–164.

Philips, D. H., 1976: A pressure jump and an associated seiche at Tobruk. *Meteor. Mag.*, **105**, 110–122.

Priestley, C. H. B., 1953: Buoyant motion in a turbulent environment. *Aust. J. Phys.*, **6**, 279–290.

Rayleigh, Lord, 1876: On waves. *Phil. Mag.*, **1**, 257–279.

Reynolds, R. M., and J. T. Gething, 1970: Acoustic sounding at Benalla, Victoria and Julia Creek, Queensland. Publ. No. 17, Meteor. Dept., University of Melbourne, Project EAR, Reps. V–VII.

Scott-Russell, J., 1837: Report on Waves. *Brit. Assoc. Rep.*, No. 417.

——, 1844: Report on Waves. *Brit. Assoc. Rep.*, No. 311.

Shaw, 1971:

Simpson, J. E., D. A. Mansfield and J. R. Milford, 1977: Inland penetration of sea-breeze fronts. *Quart. J. Roy. Meteor. Soc.*, **103**, 47–76.

Smart, E., 1966: An examination of atmospheric pressure pulses recorded on microbarographs. M.Sc. thesis, Dept. of Physics, Colorado School of Mines, Golden.

Spillane, K. T., and M. J. McCarthy, 1969: Downdraft of the organized thunderstorm. *Aust. Meteor. Mag.*, **17**, 3–24.

Stokes, G. G., 1880: On the theory of oscillatory waves. *Mathematical and Physical Papers*, Vol. 1, Cambridge University Press, 197–229, 314.

Strelkoff, T., 1971: An exact numerical solution of the solitary wave. *Proc. 2nd Int. Conf. Numerical Methods Fluid Dynamics*, Springer, 441–446.

Turner, J. S., 1963: The motion of buoyant elements in turbulent surroundings. *J. Fluid Mech.*, **16**, 1–16.

Vliegenthart, A. C., 1971: On finite-difference methods for the Korteweg-de Vries equation. *J. Eng. Math.*, **5**, 137–155.

Wallington, C. E., 1961: Observations of the effects of precipitation downdraughts. *Weather*, **16**, 35–43.

Welch, P. D., 1967: The use of fast Fourier transforms for the estimation of power spectra: a method based on time averaging over short modified periodograms. *Trans. IEEE*, **AU-15**, No. 2, 70–73.

Yamada, H., 1957: On the highest solitary wave. *Rep. Res. Inst. Appl. Mech. Kyushu Univ.*, **5**, 53–67.

——, 1958: On approximate expressions of solitary wave. *Rep. Res. Inst. Appl. Mech. Kyushu Univ.*, **6**, 35–47.

——, G. Kimura and J. Okabe, 1968: Precise determination of the solitary wave of extreme height on water of a uniform depth. *Rep. Res. Inst. Appl. Mech. Kyushu Univ.*, **16**, 15–32.

Zabusky, N. J., and M. D. Kruskal, 1965: Interaction of "solitons" in a collisionless plasma and the recurrence of initial states. *Phys. Rev. Lett.*, **15**, 240–243.